Precision Charm Decays: Leptonic, Semileptonic, Hadronic

Roy A. Briere
Carnegie Mellon University, Pittsburgh, Pennsylvania, USA

Precision results on the leptonic, semileptonic, and hadronic decays of charm mesons are reviewed. These results are important for timely progress in weak flavor physics both in their own right and as checks of theoretical calculations. Recent years have seen much progress on weak decays of charm, in both theory and experiment, a trend we expect to continue.

1. Introduction

The physics of charm mesons has been long studied for its own interesting phenomenology, as the first heavy quark. But it was, until recently, less prized for insight into weak flavor physics than the study of B physics, involving the study of the yet heavier but still accessible b quark. The higher energy scale afforded B physics a firmer theoretical base, and the surprising suppression of the leading $b \to cW^-$ decay process allows for strong displays of CP violation and neutral meson mixing. In the case of charm, less interesting Cabibbo-allowed decays dominate, making it hard to see rare processes. Charm CP violation is generally suppressed in Standard Model, as is D^0 mixing, with uncertain long-distance contributions. Experimental results are in general harder to interpret since charm is light, making calculations of QCD effects difficult. The "brown muck" of strong-interaction physics obscures the weak physics of interest. Of course, not all was bleak; there were opportunities beyond mere cataloging of charm decays. One looked for unexpected surprises, or exploited the benefits of using charm to limit new physics in the light of small Standard Model backgrounds. However, a new communal wisdom began to emerge not long ago, that charm is a gift with many uses [1].

Much of the activity in weak flavor physics involves precision measurements to over-constrain the Cabibbo-Kobayashi-Maskawa (CKM) quark mixing matrix. An inconsistency would signal new physics, and searching for such indirect evidence complements direct searches for new particles at the energy frontier. B physics experiments are the most fertile ground for these studies; they are very productive and precise, but too often limited by theory. CKM constraints are often shown as bands in a two-dimensional $(\rho - \eta)$ plane, and the widths of many of these constraint bands are limited by theory. Lattice QCD (LQCD) provides a systematic path to lift such limitations in using B results, and charm physics can be used to directly test LQCD. Of course, this is not all that charm has to offer. Recently, multiple consistent observations of D^0 mixing have enlivened this topic, as only discovery can. And analyses of charm meson Dalitz plots provide a useful tool not only for low-energy hadronic spectroscopy, but are in fact also helpful for improving precision of weak B physics results, in particular for the CKM angle *gamma*.

Here, we concentrate on precision branching fractions results which impact weak flavor physics, though we discuss some other interesting hadronic modes at the end. In particular, the increased precision of leptonic and semi-leptonic results provides a testbed for modern LQCD. If it passes, we add confidence in LQCD predictions and uncertainty estimates for B physics, where they are a critically needed compliment to pre-existing measurements of B mixing and exclusive B semileptonic decays.

Leptonic decays of $D_{(s)}$ are used to extract decay constants and the semileptonic processes $D \to K\ell\nu, \pi\ell\nu$ constrain form-factors. Golden-mode branching ratios for $D^0 \to K^-\pi^+$, $D^+ \to K^-\pi^+\pi^+$, $D_s \to K^-K^+\pi^+$ solidify the overall normalization of charm decays. Precision lifetimes, now dominated by FOCUS [2] results, are also an important input to connect theoretical partial widths to expected branching fractions. Relevant experimental techniques include tagging with near-threshold D pairs at CLEO-c and high-statistics 10 GeV data from B factories which allows for what we call "continuum tagging".

2. Experiments and Techniques

Many results have been obtained with e^+e^- collisions at threshold by CLEO-c. For D mesons, machine energies are set to produce $e^+e^- \to \psi(3770) \to D^0\bar{D}^0, D^+D^-$, while for D_s, one uses e^+e^- collision at 4170 MeV to produce $D_s^+D_s^{*-} + c.c.$ At the $\psi(3770)$, the D-pair cross-section is $\sigma(D\bar{D}) = (6.57 \pm 0.04 \pm 0.10)$ nb [3], while at 4170 MeV, $\sigma(D_s^+D_s^{*-} + c.c) = (0.916 \pm 0.011 \pm 0.049)$ nb [4]. These desired processes are in addition to a light-quark (uds) continuum cross-section of order 20 nb, plus tau pairs, radiative returns to the narrow J/Ψ and ψ', and two-photon reactions. But note that charm mesons at 3770 MeV appear *only* as $D\bar{D}$ pairs, with no room for even one fragmentation pion. On the other hand, data at 4170 MeV also includes $D\bar{D}, D^*\bar{D} + D\bar{D}^*, D^*\bar{D}^*$, and a small amount of $D_s^+D_s^-$ in addition to the desired $D_s^+D_s^{*-}$ (which is chosen due to a larger cross-section relative to the

simpler $D_s^+ D_s^-$). Kinematics can still cleanly separate these different possibilities at 4170 MeV, but the other charm and lower cross-section for the process of interest does lead to more combinatorics and decreased signal-to-noise in the D_s case.

A "tag" is simply a fully-reconstructed $D_{(s)}$ hadronic decay. A sample of tagged events has greatly reduced background and constrained kinematics, both of which aid studies of how the other $D_{(s)}$ in the event decays. One can infer neutrinos from energy and momentum conservation, allowing "full" reconstruction of (semi)leptonic decays. For hadronic branching fractions, some simple algebra will serve to demonstrate how tagged samples can provide a clean absolute normalization. The typical tag rates per $D_{(s)}$ (*not* per pair) are roughly 15%, 10%, and 5% for D^0, D^+, and D_s, respectively. CLEO-c completed data-taking in Spring, 2008, and is in the process of updating many results to the full statistics. In the meantime, the BESIII experiment at the BEPCII collider has begun its commissioning run, and their plans are to extend these methods even further.

Belle has developed tag-based techniques for use with continuum charm production from the Υ region, near 10 GeV. With hundreds of times greater charm samples, one can afford to use selected favorable semi-exclusive states which are only a small fraction of the total. This technique is exploited by Belle for (semi)leptonic decays. Partial reconstruction techniques may be used to study charm produced in B decays, a production mechanism with a rate similar to the $c\bar{c}$ continuum. A precision branching fraction result from BaBar is featured to illustrate these techniques. We will see that D^* tagging of D mesons is no longer the main workhorse.

3. Leptonic Decays and Decay Constants

Decay constants characterize the strong-interaction physics at the quark-annihilation vertex, in our case $c\bar{d}, c\bar{s} \to W^+$. In a fully leptonic decay, they parameterize all of our essential theoretical limitations. Decay constants also appear in the evaluation of box diagrams, and limit theoretical precision in calculating the neutral meson mixing. Thus, lack of knowledge of the B^0 and B_s decays constants limits the usefulness of precise measurements of $B^0 - \bar{B}^0$ and $B_s - \bar{B}_s$ oscillations. These mixing data are our best source of information on the CKM matrix elements V_{td} and V_{ts}, which are difficult to measure directly in top decay. The charm sector presents an opportunity to check LQCD results for decays against precision measurements. This is desirable since the only related direct measurement possible, the decay constant of the B^+ from measurement of $B^+ \to \ell^+ \nu$, is very challenging.

Let us first review the status in the Spring of 2008. Previous CLEO and Belle results for D_s leptonic decays averaged to give $f_{D_s} = (273 \pm 10)$ MeV [5]. The best precision claimed for LQCD, with 2+1 unquenched flavors, finds (241 ± 3) MeV [6], about a three standard-deviation discrepancy. On the other hand, D^+ results are consistent with LQCD. A 2005 CLEO f_D result of $f_D = 223 \pm 17$ MeV from 281 pb^{-1} [7], is consistent with a recent LQCD value of (207 ± 4) MeV [6]. However, in both cases, more experimental precision is clearly needed. We also await more LQCD results, to confirm the quoted results. While these results have the best claimed precision, they involve a somewhat controversial technique involving a "fourth-root trick" using computationally-efficient staggered fermions. Further details and other competing lattice results may be found in Refs. [5] and [8]. Most, but not all, have similar central values, but have larger errors due primarily to computational limitations with more traditional (but also more generally accepted) LQCD techniques.

Dobrescu and Kronfeld [9] argue that the disagreement on f_{D_S} could be the effect of new physics, mentioning both charged Higgs (their own model) and leptoquarks as possibilities. Kundu and Nandi suggest [10] R-parity violating SUSY to explain a large f_{D_s} and the B_s mixing phase.

There are now newer experimental results to report on. We first present a preliminary CLEO-c $D^+ \to \mu^+ \nu$ update using the full 818 pb^{-1} of $\psi(3770)$ data [11]. The signal side opposite the D^- tag is a single track and an unobserved neutrino. With the neutrino "detected" by four-momentum balance, one has a fully-reconstructed double-tag event: all decays products of both the D and $\bar{D}$ are measured. Mass peaks for the six hadronic tag modes are shown in Fig. 1. The chosen signal variable for the $\mu^+ \nu$ decay is the calculated square of the missing-mass of any undetected decay products, shown in Fig. 2; this should of course peak at $M_\nu^2 = 0$. The power of D-tagging is evident in the clean, isolated signal peak. The signal fit includes $K^0 \pi^+$, $\pi^+ \pi^0$, $\tau^+ \nu$ components as well. Fixing the τ-to-μ ratio at the Standard Model ratio of 2.65 gives $\mathcal{B}(D^+ \to \mu^+ \nu) = (3.82 \pm 0.32 \pm 0.09) \times 10^{-4}$ and $f_D = (205.8 \pm 8.5 \pm 2.5)$ MeV, which is the best number in context of the SM. Floating this ratio gives a consistent result of $\mathcal{B}(D^+ \to \mu^+ \nu) = (3.93 \pm 0.35 \pm 0.09) \times 10^{-4}$ and $f_D = (207.6 \pm 9.3 \pm 2.5)$ MeV; this is the best number for use with new-physics models. One sees that, in either case, this full-statistics CLEO-c result is almost twice as precise as their previous one, and remains consistent with LQCD.

Now we turn to f_{D_s}. While the Belle $D_s^+ \to \mu^+ \nu$ result from 548 fb^{-1} [12] has been out for some time, it is useful to illustrate their technique. They use "continuum tagging" with the process $e^+ e^- \to D^{\pm,0} K^{\pm,0} X D_s^{*-}$ where $X = n\pi$ or $n\pi\gamma$ (from fragmentation). About 25% of the D decay modes are used to reconstruct the tag side. The branching ratio
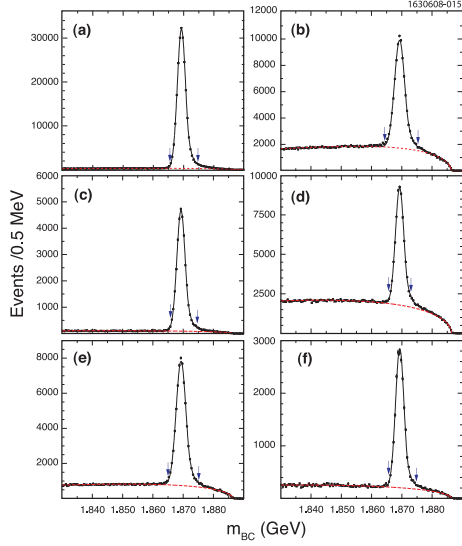
Figure 1: CLEO-c D^+ hadronic tags used for the $D^+ \rightarrow \mu^+\nu$ analysis. Modes in panels (a)−(f) are $K^+\pi^-\pi^-$, $K^+\pi^-\pi^-\pi^0$, $K_S\pi^-$, $K_S\pi^-\pi^-\pi^+$, $K_S\pi^-\pi^0$, and $K^+K^-\pi^-$, respectively.
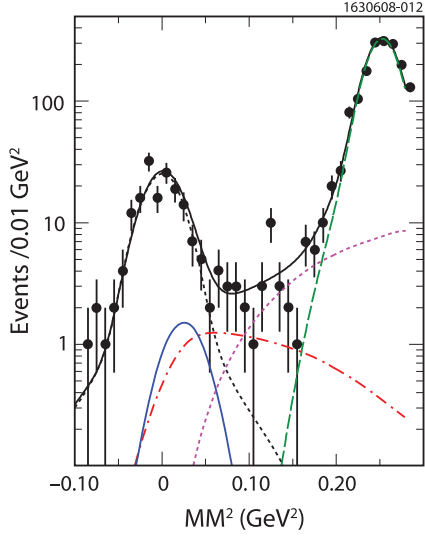

Figure 2: CLEO-c missing-mass-squared plot for $D^+ \rightarrow \mu^+\nu$; note the vertical log scale. The solid curve is a fit to the data points. Components of the fit include $\mu\nu$ signal (short-dash black), $\tau\nu$ (dot-dash red), residual $\pi^+\pi^0$ background (solid blue), $K\pi$ background (long-dash green), and other backgrounds (short-dash purple).
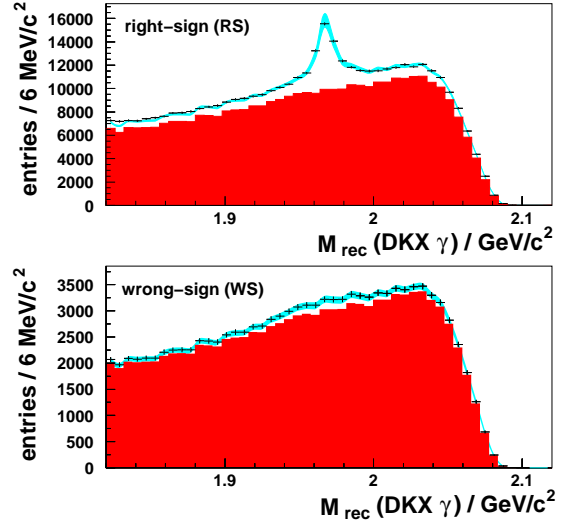

Figure 3: Recoil mass against the $DKX\gamma$ system from the Belle $D_s \rightarrow \mu\nu$ analysis. Both right-sign (RS) and wrong-sign (WS) are shown. Dark red shading shows the fitted background, while the light blue shading shows the total fit to signal and background with systematic uncertainties.
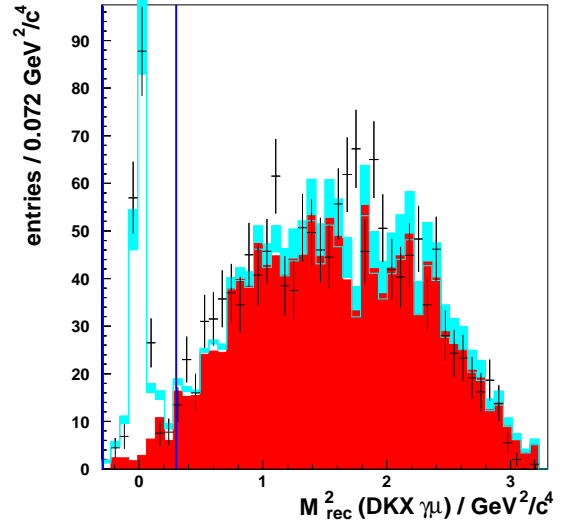

Figure 4: Recoil mass squared against the $DKX\gamma\mu$ system from the Belle $D_s \rightarrow \mu\nu$ analysis. The color scheme is the same as the previous plot. The signal region is indicated by vertical lines near zero.

of $D_s \rightarrow \mu\nu$ is proportional to a ratio of two yields, both obtained from recoil mass peaks. The recoil against $DKX\gamma$ peaks at the D_s mass, and counts the total number of D_s in their sample; see Fig. 3. The recoil against $DKX\gamma\mu$ peaks at 0 (m_ν^2), and is used to count $D_s \rightarrow \mu\nu$ decays; see Fig. 4. After some sophisticated fitting, they obtain a final result of: $\mathcal{B}(D_s^+ \rightarrow \mu^+\nu) = (0.644 \pm 0.076 \pm 0.057)\%$ and $f_{D_s} = (275 \pm 16 \pm 12)$ MeV.

CLEO-c has published an analysis of $D_s^+ \rightarrow \tau^+\nu$, with $\tau^+ \rightarrow e^+\nu\bar{\nu}$ using 298 pb^{-1} [13]. An update to the full statistics with an improved analysis is in progress. For their published analysis, only the three cleanest D_s^- tags ($\phi\pi^-, K^-K^{*0}, K^-K_S$) are used. There is always more than one neutrino, making the kinematics less well-constrained than the $\mu^+\nu$ final state. The amount of extra energy (not from the D_s^- tag or the e^+) in the calorimeter, E_{extra}, is used as
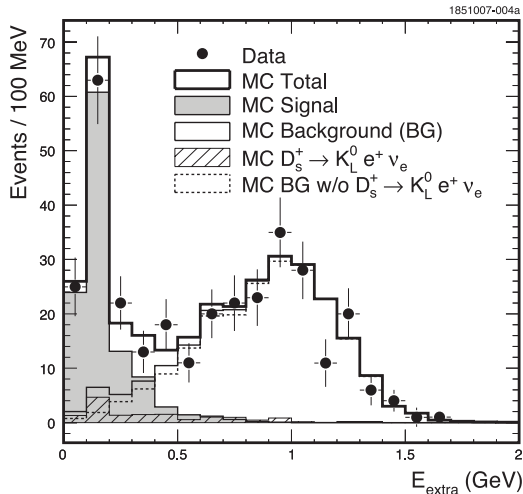
Figure 5: A plot of E_{extra} for the CLEO-c $D_s^+ \to \tau^+ \nu$, with $\tau^+ \to e^+ \nu \bar{\nu}$ analysis. E_{extra} is the energy in the calorimeter not associated with the D_s tag or the electron. Semileptonic backgrounds tend to peak away from zero. The signal peak includes cases where the 140 MeV transition photon from $D_s^* \to D_s \gamma$ is included in E_{extra}, as well as cases where it is missed.

the main signal variable; see Fig. 5. The signal region defined as $E_{extra} < 400$ MeV. Most background is from semileptonic events, which tend to have some extra energy from their hadronic daughters. Care must be taken with $D^+ \to K_L e^+ \nu$ background which peaks lower than other semileptonic modes. Note that a reconstructed γ from the $D_s^* \to D_s \gamma$ decay is not required. The final result is: $\mathcal{B}(D_s^+ \to \tau^+ \nu) = (6.17 \pm 0.71 \pm 0.34)\%$, and $f_{D_s} = (274 \pm 16 \pm 8)$ MeV.

The most precise CLEO-c results come from an analysis of $D_s^+ \to \mu^+ \nu$ and $D_s^+ \to \tau^+ \nu, \tau^+ \to \pi^+ \nu$. They are analyzed together since both contain a single track from the signal (non-tag) D_s. Note that explicit muon identification is unnecessary and would actually be inefficient at the $\mathcal{O}(1 \text{ GeV})$ energies relevant here. A published result using 314 pb^{-1} and eight hadronic decay modes is available [14]; we present here a preliminary update using ~ 400 pb^{-1} [15]. As with the D^+ analysis, the signal is studied via the missing-mass-squared; see Fig. 6. With the $\mu\nu$ to $\tau\nu$ ratio fixed at the Standard Model value in the signal fit they find: $\mathcal{B}^{\text{eff}}(D_s^+ \to \tau^+ \nu) = (0.613 \pm 0.044 \pm 0.020)$, and $f_{D_s} = (268.2 \pm 9.6 \pm 4.4)$ MeV. Fitting with both floating yields consistent results, and gives $\Gamma(D_s^+ \to \tau\nu)/\Gamma(D_s^+ \to \mu^+ \nu) = 10.3 \pm 1.1$. This is consistent with the Standard Model expectation of 9.72, and hence limits some new physics scenarios.

A new preliminary CLEO-c average of this $\mu\nu$ plus $\tau\nu, \tau \to \pi\nu$ with the previous $\tau\nu, \tau \to e\nu\nu$ result yields: $f_{D_s} = (269.4 \pm 8.2 \pm 3.9)$ MeV. A weighted average of CLEO-c and Belle gives $f_{D_s} = (269.6 \pm 8.3)$ MeV. We summarize the current situation for f_{D_s} in
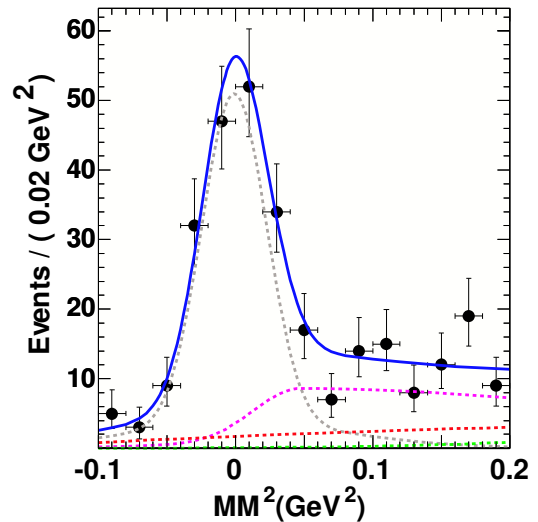

Figure 6: Missing-mass-squared plot for the CLEO-c $D_s \to \mu\nu, \tau\nu$ with $\tau \to \pi\nu$ analysis. The solid blue curve is a fit to the data points. Fit components include $\mu\nu$ signal (dashed grey), $\tau\nu$ signal (dashed purple), and two small background components (dashed green and red).

Table I. Note that a BaBar result on f_{D_s} [16] and most other older analyses all depend on $\mathcal{B}(D_s \to \phi\pi)$, and are omitted here. The roughly three standard deviation disagreement between theory and experiment for f_{D_s} still remains. Is it a problem with the theory, or experiment? A hint of new physics? Or perhaps partly an unlikely fluctuation? One must also keep in mind the excellent agreement obtained for f_D.

4. Semileptonic Decays and Form Factors

Here, strong-interaction complications are summarized by form factors, which are functions of $q^2 = M_{\ell\nu}^2$. Once again, charm offers a chance to confront LQCD calculations. Similar LQCD calculations can help us to interpret results on $B \to \pi\ell\nu$ in order to extract V_{ub}. The key charm mode for tests is $D^0 \to \pi^- \ell^+ \nu$. We discuss this and related pseudo-scalar modes; later, a new precision result on $D_s^+ \to K^+ K^- e^+ \nu$ is also featured. Form-factor normalizations can be used with external V_{cs}, V_{cd} as LQCD tests, or utilizing LQCD, for extractions of V_{cs}, and V_{cd}. We could also use ratios with leptonic decays to cancel these CKM matrix elements and test the ratio of LQCD predictions for the two types of decays. The form-factor shapes as a function of q^2 also provide direct LQCD tests. We note that $d\Gamma/dq^2$ drops rapidly due to a p^3 phase-space factor, decreasing statistics and precision at large q^2.

Belle used 282 fb^{-1} to study $D^0 \to \pi^- \ell^+ \nu, K^- \ell^+ \nu$ [17]. They use "continuum tagging" again here, ex-

Table I Summary of recent experimental results on f_{D_s}.

Experiment	Luminosity	mode	f_{D_s}
CLEO-c [15] (prelim)	$\simeq 400$ pb^{-1}	$D_s \to \mu\nu, \tau\nu(\tau \to \pi\nu)$	$268.2 \pm 9.6 \pm 4.4$
CLEO-c [13]	298 pb^{-1}	$D_s \to \tau\nu(\tau \to e\nu\nu)$	$273 \pm 16 \pm 8$
CLEO-c Average [15] (prelim)	-	-	$267.9 \pm 8.2 \pm 3.9$
Belle [12]	548 fb^{-1}	$D_s \to \mu\nu$	$275 \pm 16 \pm 12$
Current CLEO-c/Belle Average [15]	-	-	269.6 ± 8.3
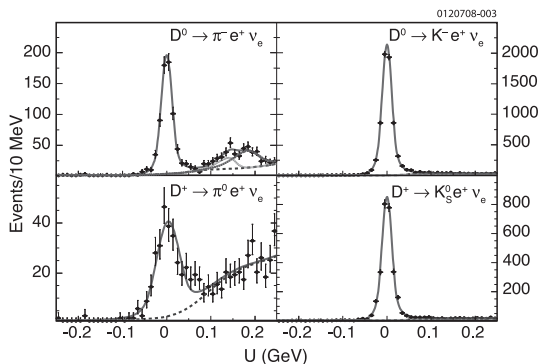
Figure 7: CLEO-c tagged semileptonic analysis signal peaks in $U = E_{miss} - p_{miss}$ for the four $Ke\nu, \pi e\nu$ modes. Notice how clean the data is, despite the neutrino.
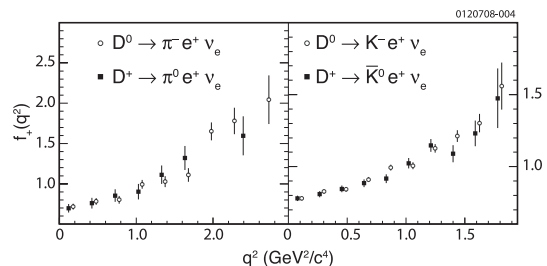

Figure 8: Form factors extracted from the CLEO-c tagged semileptonic analysis. Isospin-related modes are plotted together and agree well, as expected.

ploiting the $e^+e^- \to \bar{D}^{(*)}_{tag} D^*_{signal} X$. They reconstruct all particles, except for neutrino, and use $m^2_{miss} = E^2_{miss} - p^2_{miss}$ as their signal variable. Tagging provides absolute normalization of about 56,000 tagged D^0. The find 126 ± 12 $D^0 \to \pi^- e^+ \nu$ events, and 106 ± 12 $D^0 \to \pi^- \mu^+ \nu$ events.

CLEO-c has a published untagged analysis which uses global four-momentum balance to infer the neutrino without an explicit D tag [18]. This has about twice the efficiency of the CLEO-c simpler tagged analysis discussed next. Fitting the familiar beam-energy-constrained mass, the find 1325 ± 48 $D^0 \to \pi^- e^+ \nu$ events.

There is also a CLEO-c preliminary result also using 281 pb^{-1}, but with D tagging [19]. Signal peaks in are shown in Fig. 7 and the extracted form factors in Fig. 8. All four $Ke\nu, \pi e\nu$ modes are studied, using $U_{miss} = E_{miss} - |p_{miss}|$ as the signal variable; see Fig. 7. They find 699 ± 28 $D^0 \to \pi^- e^+ \nu$ events; threshold kinematics and tagging result in very small contamination from the ten-times more copious $K^- \pi^+ \nu$ mode. Their paper also discusses correlation and performs averages with the untagged analysis.

A more traditional $D^0 \to K^- \ell^+ \nu$ analysis was done at BaBar by tagging with $D^{*+} \to D^0 \pi^+$ [21]. While yielding very large signal statistics and an excellent analysis of $K^+ \ell^- \nu$ form factors, this technique is not well-suited to the rarer $\pi^- \ell^+ \nu$ mode. It also has somewhat poorer q^2 resolution, with unfolding needed for

the form factor measurements.

All together, significant improvements in precision have been obtained by these recent BaBar, Belle, and CLEO-c measurements. CLEO-c is the most precise for $\pi^- \ell^+ \nu$, obtaining about three times more signal events and ten times the signal-to-noise in the tagged case. Both experiments have of order three times more luminosity to analyze. Note that Belle uses electrons and muons, while CLEO-c uses only electrons. However, CLEO also does the two isospin-related modes with neutral hadrons.

We will not discuss detailed comparisons with LQCD here; some comparisons can be found in the references. Agreement is good, within current errors. Currently, normalization errors are about 10% for theory for both $Ke\nu$ and $\pi e\nu$, and are 2% and 4%, respectively, from experiment. For $Ke\nu$, a single pole model fit works reasonably well, but not with the spectroscopic D^*_s mass as the pole mass. One key issue is that fitting to a model that is not a correct description, such as a simple pole model, leads to extracted results that cannot be sensibly compared, since data points from different sources, experiments and LQCD alike, will have different precisions vs. q^2. An incorrect theory fit will be biased by preferentially accommodating the more precise points being fit. A recent influential theory paper [20] advocates using well-motivated series expansions to avoid such problems. The newer analyses (from BaBar and CLEO-c) use these expansions along with some older pole forms.

We finish with a new preliminary BaBar result on $D^+_s \to K^+ K^- e^+ \nu$ form-factors based on 214 fb^{-1} [22]. For this Cabibbo-allowed mode, high-energy con-

tinuum charm data give high statistics and are preferable to charm-threshold data. Their reconstruction technique exploits the jet structure to approximate some of the kinematics and then fits to constrain the neutrino. A detailed form-factor analysis obtains excellent angular fits to their high-statistics sample of about 25,000 events. While dominated by $D_s \to \phi e \nu$, they also find the first evidence for $D_s \to f_0 e \nu$. There is one form-factor for $f_0 e \nu$; their fit floats the intercept and the pole mass m_A. The vector ϕ meson is more complicated, requiring three form-factors for $\phi e \nu$. Their fit floats two relative normalizations using a fixed m_V as a common pole for the shape. Overall, good agreement with LQCD [23] is obtained, except perhaps for one of the normalizations in the $\phi e \nu$ case.

Some other interesting results have fallen victim to space constraints, notably inclusive branching ratios [24] as well as other exclusive branching ratios, for $D \to (\rho/\omega/\eta/K_1) e \nu$ [25].

5. Precision Hadronic Branching Fractions

We begin by explaining the tagging method used at CLEO-c. The number of "single tags" observed where a D decays in mode j is $N_j = N_{D\bar{D}} B_j \epsilon_j$; where $N_{D\bar{D}}$ is the number of $D\bar{D}$ pairs created, and $\mathcal{B}$ and ϵ are the branching fraction and efficiency. Similarly, the number of "double tags", where the D decays via mode i and the $\bar{D}$ via mode j is $N_{ij} = N_{D\bar{D}} B_i B_j \epsilon_{ij}$. Simple algebra then gives $B_i = (N_{ij}\epsilon_j)/(N_j\epsilon_{ij})$ and $N_{D\bar{D}} = (N_i N_j \epsilon_{ij})/(N_{ij}\epsilon_i\epsilon_j)$. Two key advantages are evident here. First, $\mathcal{B}_i$ independent of $N_{D\bar{D}}$ and the integrated luminosity; absolute normalization here essentially comes from the algebra. Second, one can measure cross-sections independent of branching fractions. We also note that $\epsilon_j/\epsilon_{ij} \simeq \epsilon_i$, making the branching fraction measurement almost independent of the tag mode j. This is true since we have low-multiplicity decays in a fine-grained detector. Monte-Carlo simulations are used for the signal-mode efficiency and the small effects of tag mode (the efficiency approximation noted above is *not* assumed). Systematics uncertainties are dominated by charged track, π^0, K_S, and particle identification efficiencies. It is important that D tagging techniques can also be used to explore the absolute efficiency scale with the same data sample [3]. Three D^0 and six D^+ modes are used, and results are obtained from a global fit to all single-tag and double-tag rates with correlations properly included. Their results include: $\mathcal{B}(D^0 \to K^-\pi^+) = (3.891 \pm 0.035 \pm 0.059 \pm 0.035)\%$ and $\mathcal{B}(D^+ \to K^-\pi^+\pi^+) = (9.14 \pm 0.10 \pm 0.16 \pm 0.07)\%$. Uncertainties are statistical, systematic (dominated by knowledge of absolute efficiencies), and effects of final-state radiation.
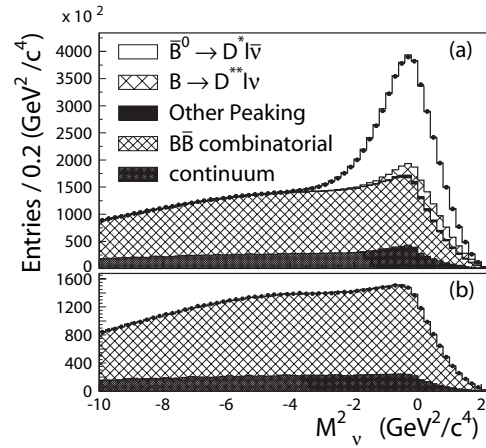

Figure 9: The missing-mass distribution from the BaBar $D^0 \to K^-\pi^+$ analysis, showing the peak from the desired $\bar{B}^0 \to D^{*+}\ell^-\nu$ process. This peak provides the normalization for the $D^0 \to K^-\pi^+$ branching ratios. Wrong-sign $D^*\ell$ pairs are also shown.
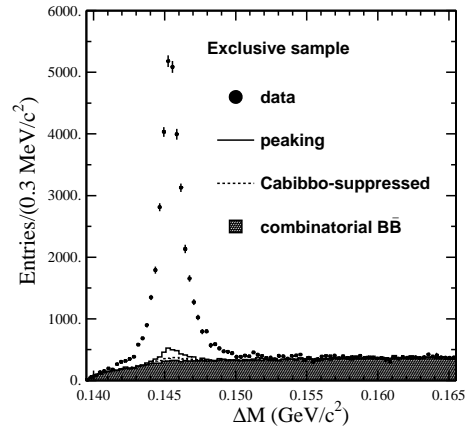

Figure 10: The BaBar $D^0 \to K^-\pi^+$ signal, shown as a peak in the $D^{*+} - D^0$ mass difference, ΔM.

BaBar has also measured $D^0 \to K^-\pi^+$ with 232 fb^{-1} of data at or near the $\Upsilon(4S)$ [26]. They employ a partial reconstruction technique for the decay $B^0 \to D^{*+}(X)l\nu$. The slow pion from the $D^* \to D^0\pi_{slow}$ decay is used to estimate the D^* momentum and calculate the missing mass without explicit reconstruction of the D^0. The resulting missing-mass peak counts the number of D^0 mesons in this inclusive sample; see Fig. 9. Full reconstruction of $D^0 \to K^-\pi^+$ is then performed within this inclusive sample to count the $D^0 \to K^-\pi^+$ decays; see Fig. 10. $\mathcal{B}(D^0 \to K^-\pi^+) = (4.007 \pm 0.037 \pm 0.072)\%$. Systematics of 1.8% primarily come from 1.5% uncertainty on the exclusive efficiency and 1.0% for the inclusive efficiency.

The golden D^+ mode is now measured to 2.2% by CLEO-c, the best previous single measurements had errors larger than 10%. The golden D^0 mode is now
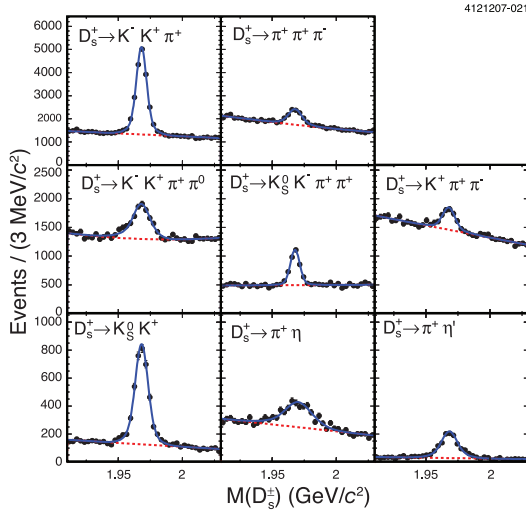
Figure 11: CLEO-c D_s mass peaks for hadronic single-tag modes used in the branching fraction analysis.

Figure 12: Summary of CLEO-c D_s branching ratio results compared to previous world averages.

determined to about 2% by both CLEO-c and BaBar; the best previous measurements had errors greater than 3.6%. Both of these key modes are now systematics limited.

More recently, CLEO-c reported hadronic branching fractions for several D_s decays, based on 298 pb^{-1} of data at $E_{cm} = 4170$ MeV [27]. Single-tag mass peaks for the eight D_s decay studied are shown in Fig. 11. Their sample of about $N_{DT} = 1000$ double tags sets the scale of achievable statistical uncertainties as $\geq 1/sqrtN_{DT}$. We point out that the historical use of $D_s^+ \to \phi\pi^+$ as the mode of choice for D_s normalization has some problems. It is difficult to cleanly define what "ϕ" means given other nearby resonances (such as the f_0) and interference between various contributions to the $K^+K^-\pi^+$ final state. These effects change the angular distributions in the ϕ mass region, complicate separation of *phi* and non-*phi* contributions, and lead to dependence on experimental resolution. Thus, CLEO-c quotes a result for the entire phase-space: $\mathcal{B}(D_s \to K^+K^-\pi^+) = (5.50 \pm 0.23 \pm 0.16)\%$. They also quote $\mathcal{B}(D_s \to K^+K^-\pi^+)$ within various K^+K^- mass windows, which are related to some sort of "$\phi\pi^+$" branching ratio. In Fig. 12, we illustrate the improvements over previous world averages achieved by these new results. The full data sample will more than double the statistics.

While we have concentrated here on golden-mode branching fractions for D^0, D^+ and D_s, many other results such as Cabibbo-suppressed final states and inclusive branching fractions have also been explored [2].
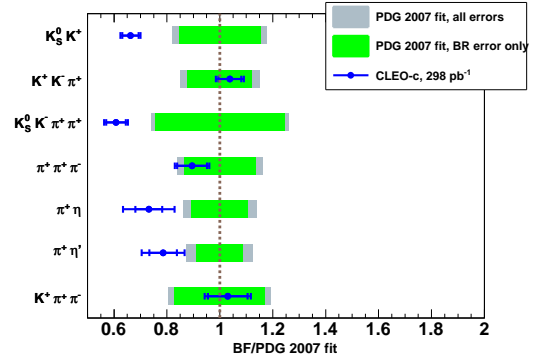
6. Other Hadronic Results

We start with some of the unique opportunities available at CLEO-c due to quantum correlations between the $D\bar{D}$ pairs produced at the $\psi(3770)$. This is used, for example, to measure the strong $K\pi$ final-state interaction (FSI) phase with 281 pb^{-1} [28]. This is of great interest for interpreting D mixing results based on the $D^0 \to K^-\pi^+$ mode, which are contaminated by this FSI phase. Results are extracted from a simultaneous fit to their data on many hadronic (both flavor and CP eigenstates) and semileptonic modes, plus external inputs from D mixing measurements. For the experts, these external inputs are x, y, x', y', r^2. They find: $cos\delta = 1.10 \pm 0.35 \pm 0.07$, $\delta = (22^{+11+9}_{-12-11})°$. Note that the most likley $\cos\delta$ is in general *not* the cosine of the most likely δ, due to a $d\cos\delta/d\delta$ factor when changing the abscissa.

CLEO-c has also investigated interference in $K_L\pi, K_S\pi$ final states. D decay diagrams can produce both K^0 and $\bar{K}^0$; these interfere in physical K_L, K_S final states, which leads to a K_S, K_L asymmetry [29]. For $D^0 \to K_{S,L}\pi^0$, we expect an asymmetry of $R(D^0) = 2\tan^2\theta_C \sim 10\%$. For the $D^+ \to K_{S,L}\pi^+$ case, there are more diagrams to consider and predictions take more work. CLEO-c results are obtained from 281 pb^{-1} are [30]; they find $R(D^0) = 0.108 \pm 0.025 \pm 0.024$, consistent with $2\tan^2\theta_C$. For the D^+, they quote $R(D^=) = 0.022 \pm 0.016 \pm 0.018$. In this case, D.-N. Gao predicts $R(D^+) = 0.035 \leftrightarrow 0.044$ [31], while Bhattacharya and Rosner predict $R(D^+) = 0.006^{+0.033}_{-0.028} \pm 0.007$ [32].

We close with a novel result; CLEO-c has measured $\mathcal{B}(D_s \to p\bar{n}) = (1.30 \pm 0.36^{+0.12}_{-0.16}) \times 10^{-3}$ [33]. Well-identified protons are combined with D tags to calculate a missing-mass which cleanly peaks at the neutron mass. This is the first observation of a charmed meson decaying into a baryon-antibaryon final state.

7. Conclusions

Many recent experimental charm results have been reviewed, and the progress of recent years is continuing. Tests of Lattice QCD are becoming more becoming precise, and there is currently an intriguing disagreement for f_{D_s} even as f_D matches very well. Charm threshold data is generally best for experimental precision, but significant contributions are also made from other experiments. Much existing data left to mine at BaBar, Belle, CLEO. Very soon we will have data from BESIII and LHC-b, and likely a Super-B factory will follow as well. In parallel, lattice QCD marches onwards with more CPU and new techniques. All in all, charm is alive and well, complimenting and extending B physics.

Acknowledgments

References

1 See, for example, S. Bianco, F.L. Fabbri, D. Benson, and I. Bigi, Nuovo Cimento, **26**, 1 (2003).

2 Review of Particle Physics, C. Amsler, *et al.*, Phys. Lett. **B 667**, 1 (2008).

3 CLEO Collaboration, S. Dobbs *et al.*, Phys. Rev. **D 76**, 112001 (2007).

4 CLEO Collaboration, D. Cronin-Hennessy *et al.*, arXiv:0801.3418 (submitted to Phys. Rev. D.).

5 J. Rosner and S. Stone, in *Decay Constants of Charges Pseudo-Scalar Mesons*, a topical review contained in Ref. [2].

6 E. Follana, C.T.H. Davies, G.P. Lepage, and J. Shigemitsu (HPQCD and UKQCD Collaborations), Phys. Rev. Lett. **100**, 062002 (2008).

7 CLEO Collaboration, M. Artuso *et al.*, Phys. Rev. Lett. **95**, 251801 (2005).

8 Lattice 2008 Symposium, Williamsburg, VA, USA; http://conferences.jlab.org/lattice2008/ .

9 B.A. Dobrescu and A.S. Kronfeld, Phys. Rev. Lett. **100**, 241802 (2008).

10 A. Kundu and S. Nandi, Phys. Rev. **D 78**, 015009 (2008).

11 CLEO Collaboration, B.I. Eisenstein *et al.*, arXiv:0806.2112, to appear in Phys. Rev. **D**. Numbers quoted here differ from preliminary ones presented at the conference (by < 1 MeV) due to inclusion of radiative corrections.

12 Belle Collaboration, L. Widhalm *et al.*, Phys. Rev. Lett. **100**, 241801 (2008).

13 CLEO Collaboration, K.M. Ecklund *et al.*, Phys. Rev. Lett. **100**, 161801 (2008).

14 CLEO Collaboration, M. Artuso *et al.*, Phys. Rev. Lett. **99**, 071802 (2007); CLEO Collaboration, T.K. Pedlar *et al.*, Phys. Rev. **D76**, 072002 (2007).

15 Sheldon Stone, arXiv:0806.3921 (presentation at FPCP 2008, Taipei).

16 BaBar Collaboration, B. Aubert *et al.*, Phys. Rev. Lett. **98**, 141801 (2007).

17 Belle Collaboration, L. Widhalm *et al.*, Phys. Rev. Lett. **97**, 061804 (2006).

18 CLEO Collaboration, D. Cronin-Hennessy *et al.*, Phys. Rev. Lett. **100** 251802 (2008); CLEO Collaboration, S. Dobbs *et al.*, Phys. Rev. **D 77** 112005 (2008).

19 CLEO Collaboration, J. Y. Ge *et al.*, to be submitted to Phys. Rev. **D**.

20 T. Becher and R. Hill, Phys. Lett. **B 633**, 61 (2006); see references therein for related previous work by others.

21 BaBar Collaboration, B. Aubert *et al.*, Phys. Rev. **D 76**, 052005 (2007).

22 BaBar Collaboration, B. Aubert *et al.*, arXiv:0807.1599, submitted to Phys. Rev. **D**.

23 J. Gill (for UKQCD Collaboration), Nucl. Phys. Proc. Suppl. **106**, 391 (2002).

24 CLEO Collaboration, N.E. Adam *et al.*, Phys. Rev. Lett. **97**, 251801 (2006).

25 CLEO Collaboration, R.E. Mitchell *et al.*, submitted to Phys. Rev. Lett.

26 BaBar Collaboration, B. Aubert *et al.*, Phys. Rev. Lett. **100**, 051802 (2008).

27 CLEO Collaboration, J. Alexander *et al.*, Phys. Rev. Lett. **100**, 161804 (2008).

28 CLEO Collaboration, J.L. Rosner *et al.*, Phys. Rev. Lett. **100**, 221801 (2008); CLEO Collaboration, D.M. Asner *et al.*, Phys. Rev. **D 78**, 012001 (2008).

29 I. Bigi and H. Yamamoto, Phys. Lett. B **349**, 363 (1995).

30 CLEO Collaboration, Q. He *et al.*, Phys. Rev. Lett. **100**, 091801 (2008).

31 D.-N. Gao, Phys. Lett. B **645** 59, (2007).

32 B. Bhattacharya and J.L. Rosner, Phys. Rev. D **77**, 114020 (2008).

33 CLEO Collaboration, S.B. Athar *et al.*, Phys. Rev. Lett. **100**, 181802 (2008).